PAPER

Alignment of carbon iron into polydimethylsiloxane to create conductive composite with low percolation threshold and high piezoresistivity: experiment and simulation

To cite this article: Shuai Dong and Xiaojie Wang 2017 *Smart Mater. Struct.* **26** 045027

IOP Publishing Smart Materials and Structures
Smart Mater. Struct. **26** (2017) 045027 (11pp) https://doi.org/10.1088/1361-665X/aa62d2

Alignment of carbon iron into polydimethylsiloxane to create conductive composite with low percolation threshold and high piezoresistivity: experiment and simulation

Shuai Dong[1,2] **and Xiaojie Wang**[2]

[1] Department of Precision Machinery and Precision Instrumentation, University of Science and Technology of China, Hefei 230026, People's Republic of China
[2] Institute of Advanced Manufacturing Technology, Hefei Institutes of Physical Science, Chinese Academy of Sciences, Changzhou 213164, People's Republic of China

E-mail: xjwang@iamt.ac.cn

Received 21 December 2016, revised 15 February 2017
Accepted for publication 24 February 2017
Published 14 March 2017

Abstract

In this study, various amounts of carbonyl iron particles (CIPs) were cured into polydimethylsiloxane (PDMS) matrix under a magnetic field up to 1.0 T to create anisotropy of conductive composite materials. The electrical resistivity for the longitudinal direction was measured as a function of filler volume fraction to understand the electrical percolation behavior. The electrical percolation threshold (EPT) of CIPs–PDMS composite cured under a magnetic field can be as low as 0.1 vol%, which is much less than most of those studies in particulate composites. Meanwhile, the effects of compressive strain on the electrical properties of CIPs–PDMS composites were also investigated. The strain sensitivity depends on filler volume fraction and decreases with the increasing of compressive strain. It has been found that the composites containing a small amount of CI particles curing under a magnetic field exhibit a high strain sensitivity of over 150. Based on the morphological observation of the composite structures, a two-dimensional stick percolation model for the CIPs–PDMS composites has been established. The Monte Carlo simulation is performed to obtain the percolation probability. The simulation results in prediction of the values of EPTs are close to that of experimental measurements. It demonstrates that the low percolation behavior of CIPs–PDMS composites is due to the average length of particle chains forming by external magnetic field.

Keywords: conductive composite, polydimethylsiloxane, carbon iron, alignment, percolation threshold, piezoresistivity

(Some figures may appear in colour only in the online journal)

1. Introduction

A conductive composite consists of two parts: one is the insulated polymer matrix, and the other is the conductive filler. These composites possess the properties of both metals and polymers which are conductive and flexible. Fillers inside the matrix can be randomly distributed or be aligned. When the filled particles are magnetizable materials, one way to produce aligned conductive composites is to apply a magnetic field during the curing process. This method creates a force between the fillers that induces the magnetic fillers to arrange in the direction of the magnetic field into chain-like structures. The chain-like structures significantly improve the electrical conductivity of the composites. The electrical properties of

Table 1. Results of conductive composites in previous studies.

Authors	Material composition	Modulus Mpa	Gauge factor $(\Delta R/R_0)/\varepsilon$
	Isotropic		
Ghafoorianfar *et al* [6]	CI-SR	20	50
Abyaneh and Kulkarni [9]	Zn-PDMS	30	30
Abyaneh *et al* [10]	Cu-PDMS	80	30
	Ni-PDMS		160
Bloor *et al* [12]	Ni-SR	20	33
Shang *et al* [13, 14]	Ni-SR	20	180
Jung *et al* [11]	Cu-PDMS	80	32
	Anisotropic		
Wang *et al* [7]	CI-SR	2	5
Bica *et al* [8]	CI–Graphene-SR	2	95
Mietta *et al* [15, 16]	Fe_3O_4@Ag-PDMS	10	140
Jang and Yin [17]	Ni-MWCNTs-PDMS	20	80

* SR: silicon rubber, CI: carbon iron, Fe_3O_4@Ag: Fe_3O_4 particles coated with Ag, MWCNTs: multi-wall carbon nanotubes.

the composites depend on the volume fraction of the fillers, the intensity of the magnetic field during the curing process and the mechanical conditions (such as uniaxial stress). As the conductive particle-filled composites exhibit a high strain capacity and excellent electrical properties, applications of conductive composites can be found in broaden areas such as an artificial skin and a robotic haptic sensing system [1–3]. In addition, a few studies have shown that when the conductive fillers incorporated into a shape-memory polymer the composites exhibits rapid electrical actuation capabilities due to the synergistic effect of the thermal and electrical properties [4, 5].

There is a critical particle volume fraction (referred to as electrical percolation threshold (EPT)), at which the conductivity of the conductive composites rapidly increases by many orders of magnitude. The percolation threshold is extremely sensitive to the conducting particle volume fraction and structures. In previous studies, conductive composites filled with CI [6–8], Zn [9], Cu [10, 11], Ni [12–14] and Fe3O4@Ag [15, 16] particles were produced and tested. The isotropic composites have very high percolation threshold (>20 vol% in general). In order to achieve a good conductivity of the composites, polymer matrix should be filled with a large amount of particles that lead to higher cost and poor mechanical properties. Thus, reducing amount of the conductive fillers has technological advantages in preparing conductive composites. In recent studies, a magnetic field was applied to cure the magnetic particles filled composites to produce anisotropic conductive composites where the percolation threshold was reduced significantly. Boudenne *et al* [18] prepared anisotropic Ni–silicone composites in a magnetic field and reduced the percolation threshold from 25 to 2 vol%. Goc *et al* [19] experimentally and Jang *et al* [20] theoretically confirmed that the average length of the chains formed by ferromagnetic particles increased with the increase of the magnetic field. Their studies implied that it is possible to control the conductivity of ferromagnetic particles filled composites by adjusting the external magnetic field during the curing process. However, the piezoresistive properties of the anisotropic composites are not as good as expected. The piezoresistive effect of a material is described by its gauge factor, which is defined as relative change in electrical resistivity per mechanical strain. The larger the gauge factor is, the more sensitivity of the materials in response to mechanical deformation. The results are reviewed and listed in table 1.

In addition to align the magnetic spherical particle within polymer matrix, the stick-like conductive fillers were also used to generate low EPT conductive composites. It is easy to understand that the stick-like fillers are preferred to form conductive networks than the spherical fillers at low amount [21, 22]. White *et al* [23] and Gelves *et al* [24] prepared ECCs filled with conductive Ag nanowires and Cu nanowires, and the EPTs were significantly reduced to 2.3 vol% and 0.5 vol%, respectively. The low EPTs could be attributed to the high aspect ratio and the distribution of stick-like conductive fillers. It could be considered that the percolation occurred when the conductive fillers dispersed well in the matrix formed the first conductive network. Similarly, carbon nanotubes (CNTs) had attracted significant interest because of their small size, large aspect ratio and high electrical conductivity. Thus far, studies on the conductive CNTs filled ECCs [25–29] have been performed and EPTs were obtained from less than 0.01 [25] to 1 vol% [27]. The dispersibility of CNTs in polymer matrix would take great influence on the EPTs while well dispersed CNTs was important for obtaining low EPTs. Unfortunately, CNTs tended to aggregate during the fabrication of composites.

On account of the difficulty in fully controlling the shape, length and dispersion of stick-like fillers in experiments, the EPTs of sticks filled ECCs were commonly researched by Monte Carlo simulation methods [23, 30–36]. As reported in the previous studies, the aspect ratio [19–35] and the angular distribution [34–36] of the stick-like fillers were the

Table 2. Material components.

CIPs volume fraction %	PDMS-A g	PDMS-B g	CIPs g
0.1	10	1	0.072
0.2	10	1	0.144
0.5	10	1	0.362
1.0	10	1	0.727
2.0	10	1	1.469
5.0	10	1	3.787

predominant influences on the EPTs. The EPTs reduced with the increase of the aspect ratio [23, 29, 34, 35].

In this paper, we proposed a way to prepare carbonyl iron particles-polydimethylsiloxane (CIPs–PDMS) composites with a very low EPT by applying an external magnetic field on the CIPs during curing process. The CIPs form chain-like structures inside the matrix, and the CIPs–PDMS composites could be regarded as a stick percolation system. The strength of magnetic fields on the average length of the CIP chains is investigated by morphological method. The effects of filler volume fraction, the intensity of applied magnetic field and mechanical strain on resistivity of the samples are also studied. The EPTs are obtained by fitting the experimental data to the statistical percolation power law. A simplified two-dimensional stick percolation network model based on the CIP chain-like structures is proposed and Monte Carlo simulations are performed to predict the EPT in comparing with the experimental results.

2. Materials and experimental study

2.1. Preparation of the CIPs–PDMS composites

The materials used to obtain the conductive composites include carbon iron particles (Jiangsu Tianyi Ultra-fine metal powder Co., Ltd, China) and polydimethylsiloxane (Sylgard 184, Dow Corning, USA). The diameter of the carbon iron particles (referred to as CIPs) ranges from 1.0 to 3.0 μm. The polydimethylsiloxane (referred to as PDMS) is made up of two parts: PDMS-A and PDMS-B. Moreover, PDMS-B could be regarded as a curing agent.

In the first step, PDMS-A and PDMS-B were mixed in proportion of 10:1 in weight at room temperature and then loaded with the CIPs. The amount of PDMS and CIPs were weighed during mixing on an analytical balance, and the details for different samples are listed in table 2. The mixture was mechanical stirred for 10 min and was dispersed in an ultrasonic dispersion instrument for 10 min. There were lots of air bubbles in the mixture, so it was necessary to put the mixture into a vacuum drying oven to remove the air bubbles.

In the second step, the mixture was poured into an aluminum mold (45 mm in length, 30 mm in width, 2 mm in thickness), and removed the air bubbles generated in the process, then sealed the mold. Finally, as shown in figure 1, the mold was placed in an electromagnet which can provide highly homogeneous, steady magnetic field up to 1.5 T. The CIPs aggregated along the direction of the magnetic field into special chain-like structures. The intensity of the magnetic field changed with the supply current. The intensity of the uniform magnetic field (H_{curing}) used in producing the CIPs–PDMS composites were 0.2 T, 0.5 T and 1.0 T respectively. A Gauss meter (BST 200, Hangzhou Parfi technology Co., Ltd, China) was used to test the intensity of the magnetic field. Furthermore, the mold was heated to a temperature of over 80° centigrade by a ceramic heating element. The mixture cured into an anisotropic CIPs-PDMS composite sample in about 2 h.

2.2. Morphology of the CIPs–PDMS composites

The morphology of the CIPs–PDMS composites was studied using a field emission scanning electron microscope (FESEM, SUPRA 55, Germany). The samples were brittle fractured in liquid nitrogen, then the SEM images were obtained observing the cross sections. As shown in figure 2(a), the CIPs were arranged in the direction of the magnetic field to generate conductive chains varied in lengths. The diameters of the CIPs distributed from 1 to 3 μm, and the adjacent particles moved close to each other under the action of the magnetic field (shown in figures 2(b) and (c)). As shown in figure 2(d), the CIPs were coated by the polymer matrix but not directly contacted with each other.

2.3. Percolation properties of the CIPs–PDMS composites

A high resistance/micro current measuring instrument (EST 121, Beijing Electro-Static Test Co., Ltd, China) was used for the voltammetry measurements. The electrical responses of the CIPs–PDMS composites to the applied voltage were measured, and the voltage–current curves of the CIPs–PDMS samples with different CIP volume fractions were obtained. In the measurement, the CIPs–PDMS composites were cut into small samples with 20 mm in length, 20 mm in width and 2 mm in thickness. Two-point contact direct-current (dc) conductivity measurement was applied to these tests since the resistances of the samples were in a high range from $\sim 1 \times 10^3$ to $10^{12}\,\Omega$. As shown in figure 3, the samples were attached between two thin square copper electrodes with thickness of 0.1 mm in the center. The electrodes were selected thin enough to make sure that they touched the surfaces of the samples well. Moreover, the samples with copper electrodes linked to the EST 121 were repeatedly compressed and released for 10 times to ensure that the samples and the electrodes were reliably adhesive before the electrical resistivity tests.

To evaluate the electric anisotropy of the CIPs–PDMS composites, electrical resistivity ρ (Ω cm) were obtained in the curing direction of applied magnetic field as a function of the volume fraction φ of the CIPs. Considering the effect of the magnetic field strengths on the electric anisotropy, samples with various particle components were prepared under magnetic fields of 0.2 T, 0.5 T and 1.0 T respectively. For all samples, the electrical resistivity was measured with a pre-compression force of $\sim$1 N to make sure the electrodes and the samples contacting tightly. The variations of ρ versus

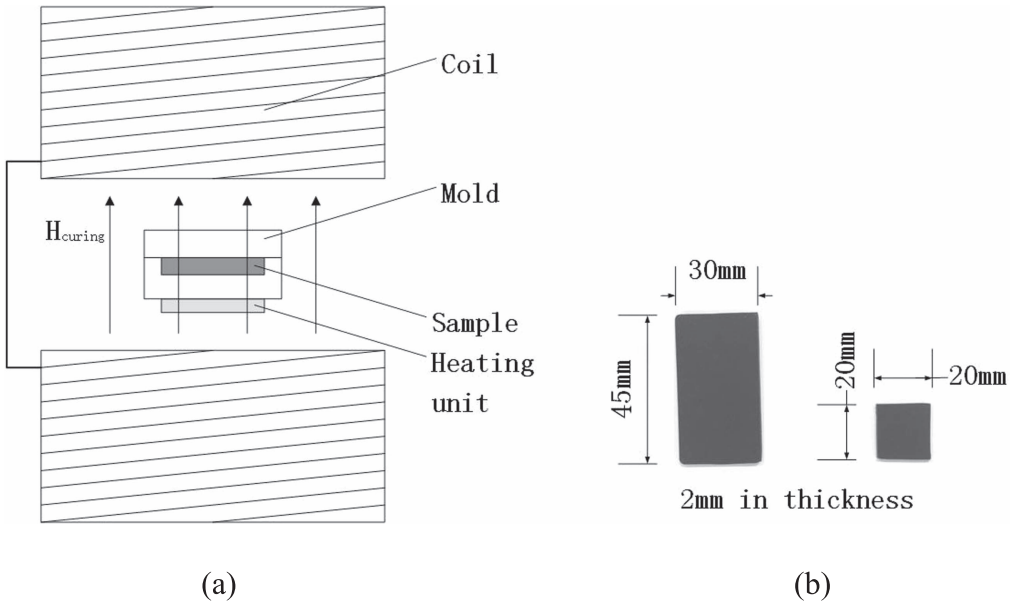

Figure 1. (a) Schematic illustration of the curing process. (b) Pictures of the samples.

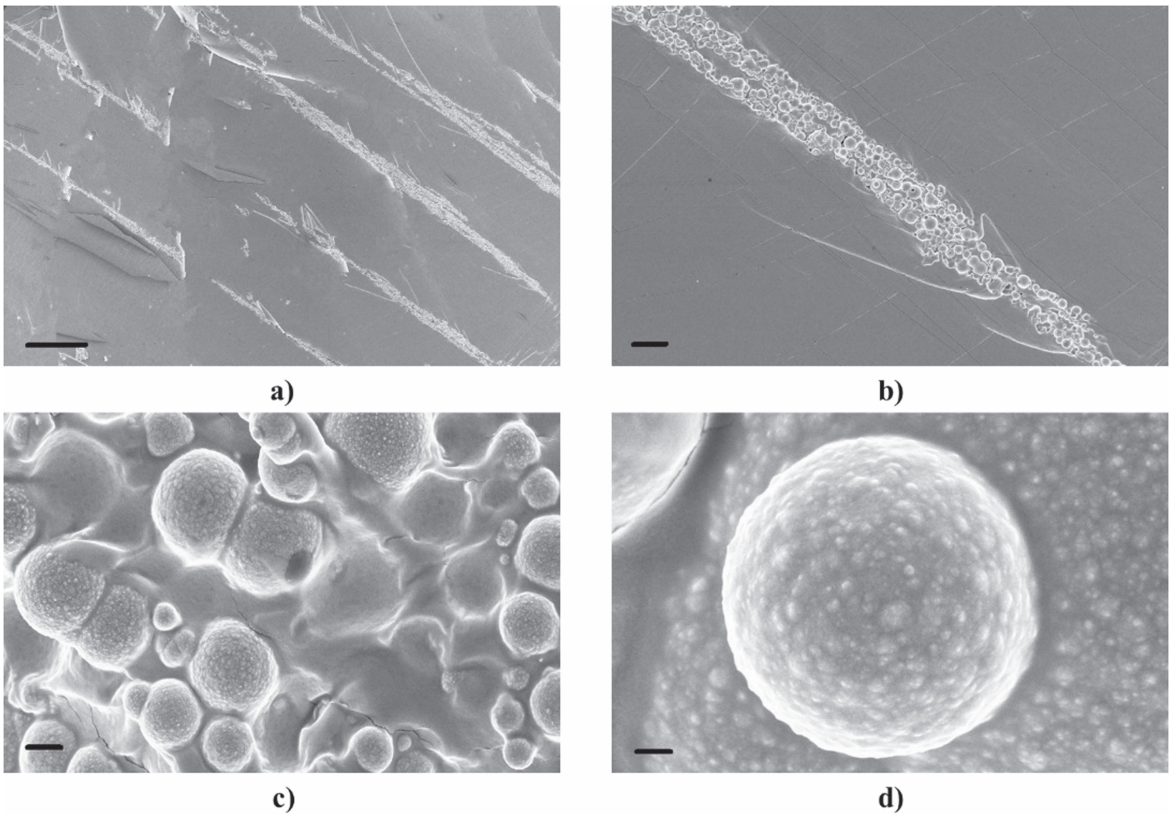

Figure 2. (a) Lateral view showing the CIPs chains. (b) and (c) images focus on one chain. (d) Magnified view of a CIP coated by polymer matrix. The scale bars are (a) 100 μm, (b) 10 μm, (c) 1 μm, (d) 200 nm.

particle volume fraction φ were shown in figures 6(a)–(c). The EPTs were obtained by fitting the experimental data to the statistical percolation power law:

$$\rho \propto (\varphi - \varphi_c)^{-t}, \quad (1)$$

where ρ is the electrical resistivity, φ_c is the EPT (i.e. the critical concentration of CIPs needed to establish a continuous conductive network), t is the critical exponent. As shown in figure 4(d), the EPTs of the samples cured under a magnetic field of 0.2 T, 0.5 T and 1.0 T were obtained as 1.49 vol%, 0.29 vol% and 0.10 vol%, respectively. It is obvious that the stronger the curing magnetic field is applied, the lower of the EPT is. This phenomenon may due to the strength of magnetic field affecting the formation of the CIP chains. Higher

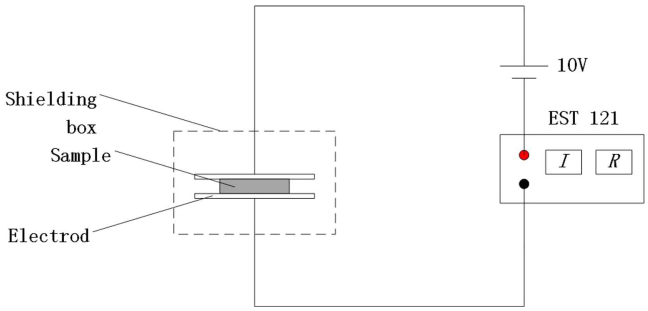

Figure 3. Schematic illustration of the electrical resistivity test.

magnetic field makes more CIPs aggregating in the direction of field; as a result, longer particle chains forms. The longer chains are more likely to establish a continuous conductive network with lower CIPs volume fraction. The EPT as low as 0.10 vol% was obtained while preparing CIPs–PDMS composite samples curing under magnetic field of 1.0 T, which has not been observed in spherical particles filled conductive composites.

2.4. Piezoresistive properties of the CIPs–PDMS composites

As reported in previous studies, the electrical resistivity of conductive composites was extremely sensitive when the filler content was around the EPT, in which a high piezoresistivity of conductive composites could be achieved [9, 15]. Therefore, in this study, we investigated the piezoresistive properties of the CIPs–PDMS composites at particle volume fractions of 0.1, 0.2, 0.5 vol% when the samples were cured under 1.0 T (the EPT = 0.10 vol%) and 1.5, 3.0, 5.0 vol% when the samples were cured under 0.2 T (the EPT = 1.49 vol%). The piezoresistivity of the CIPs–PDMS composites were obtained by measuring the electrical resistances R along the direction of the particle chains versus the applied normal stress. The relative resistance changes of the CIPs–PDMS samples with different particle volume fractions were plotted as a function of the applied stress as shown in figure 5(a). All the samples were cured under a magnetic field of 0.2 T. It shows that the relative resistance change, defined as $\Delta R/R_0$, increases rapidly while the stress σ increases from 0 to ~50 kPa. However, the relative resistance changes much slower when the stress is over 50 kPa. Accordingly, the gauge factors defined as $(\Delta R/R_0)/\varepsilon$, are plotted versus mechanical strain shown in figure 5(b). It is clear to see that the gauge factors are depended on the applied mechanical strain ε. The gauge factor is higher than 150 for the strain $\varepsilon < 0.01$, which means the electrical resistivity of the CIPs–PDMS composites is very sensitive to small deformation. On the other hand, the gauge factor decreases rapidly with increase of the strain. Similar results are observed in the CIPs–PDMS composites cured under the magnetic field of 1.0 T, which are shown in figures 5(c) and (d). Comparing figures 5(b) and (d), a higher gauge factor is obtained for the sample with 1.5 vol% particle volume fraction cured under magnetic field of 0.2 T within the strain range $0 < \varepsilon < 0.01$. The increase of the content of CIPs in a certain range may contribute to the large gauge factor.

3. Observation and simulations

In previous section we had experimentally demonstrated that alignment of CIPs into PDMS can create conductive composite with low percolation threshold and high piezoresistivity. In this section, we will employ statistical method to obtain average lengths of the particle chains of the CIPs–PDMS composites for different magnetic fields. These results are very useful to build the two-dimensional stick percolation model for the CIPs–PDMS composites. Then we will show that the electrical percolation behavior of the CIPs–PDMS composites cured under a magnetic field can be explained by the two-dimensional stick percolation model.

3.1. Chain-like structures of the CIPs–PDMS composites

The special chain-like structures of the CIPs in polymer matrix had a significant impact on electrical property of the CIPs–PDMS composites. A polarization microscope (POM) was used to observe the details of the CIP chain-like structures. Firstly, the composites were cut into non-opaque slices along the direction of the CIP chains. Then set the POE's magnification and aperture to get clear images of the CIP chains. To understand the percolation behavior of the aligned CIPs–PDMS composites, the most important of this morphology study is observing the lengths and the intersections of the CIP chains inside the PDMS when cured under different magnetic field.

Once the magnetic field was applied, a force generated between the CIPs which was in proportion to the intensity of the magnetic field. Then the adjacent particles moved close to each other under the effect of the force to make chain-like structures along the magnetic field line. But as we can see in figure 6, the CIP chains were not fully parallel to the magnetic field line. There was a small angle θ between the CIP chains and the magnetic field line, and the angle in this experiment had been found less than 5°. This result was also obtained in the work of Mietta *et al* [34]. More important, the length of the CIP chains varied in a certain range. The morphology of the CIP chains was determined by the intensity of the magnetic field, which was also discussed in some previous work [19, 20]. There were more CIP chains in the composites cured in 0.2 T, but the lengths of the chains were much smaller compared with that in composites cured in 1.0 T. To evaluate the length distributions of the CIP chains in the CIP–PDMS composites, dozens of POE images were obtained at the magnification of 100×. The real lengths of the CIP chains could be simply calculated according to the scale bar. Lengths of 170 chains and 135 chains were counted for samples cured under 0.2 T and 1.0 T magnetic field respectively. Figure 7(a) shows the histogram obtained for the length distribution of the chains formed in 0.2 T magnetic field. The average length $\langle l \rangle$ of the chains can be obtained by a Gaussian distribution function fitting the histogram, which is 0.71 mm.

A similar process applying on the samples cured under 1.0 T magnetic field, we obtained the average length is 1.14 mm, as shown in figure 7(b). These results are very close to the work of Mietta *et al* [34], who studied the structured

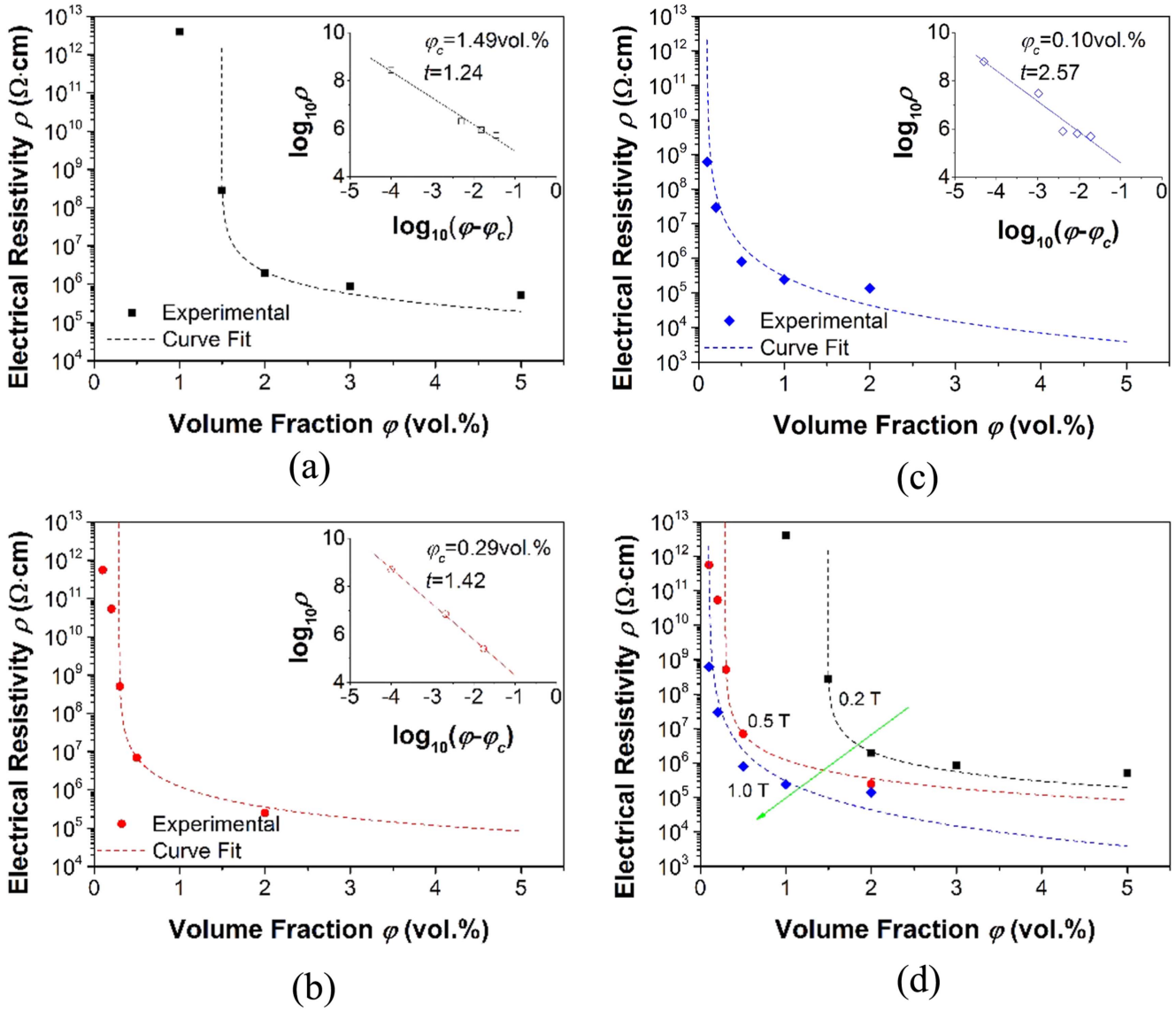

Figure 4. Electrical resistivity of the CIPs–PDMS composites as a function of CIP volume fraction. (a) cured in 0.2 T, (b) cured in 0.5 T, (c) cured in 1.0 T. Inset: $\log_{10}\rho$ versus $\log_{10}(\varphi - \varphi_c)$, the solid line represents the model fit given by equation (2). (d) Comparison of the three EPTs.

magnetorheological elastomer (MRE) composite with magnetic Fe_3O_4 silver-covered micro-particles in PDMS.

3.2. Algorithm and simulations

Within the polymer matrix, the CIPs arrange into chains with a certain length distribution, and a continuous conductive network may get formed by connections among these chains, as a result the electric percolation occurs. To understand the percolation behavior of the aligned CIPs–PDMS composites, the formation of conductive networks in composites can be evaluated by Monte Carlo simulations. In the 2D simulation cell a number of CIP chains described as line segments with a certain length distribute regularly. Each line segment can be considered as an ideal electrical conductor. Furthermore, an intersection of two line segments can be seen as a perfect conductive junction. It can be determined whether a spanning conductive network emerges connecting two opposite edges of the cell and thereby yields a percolation behavior.

Each simulation consists of, starting with an empty square cell (side $a = a_x = a_y = 2$ mm), adding a number N_{chain} of line segments of length L, and determining whether there is a spanning network between the opposite edges of the cell. Once the line segments have been generated in the cell, we should determine which line segments intersect. Let A_i and B_i indicate the end points of the line segments, $i = 1, 2,\ldots, N_{\text{chain}}$, thus the line segments can be considered as vectors, A_iB_i. Consider the positional relationship of two line segments, A_1B_1 and A_2B_2. They intersect if the following conditions both are satisfied [34]:

$$\begin{aligned}(\overrightarrow{A_1B_1} \times \overrightarrow{A_1A_2}) \cdot (\overrightarrow{A_1B_1} \times \overrightarrow{A_1B_2}) \leqslant 0\\ (\overrightarrow{A_2B_2} \times \overrightarrow{A_2A_1}) \cdot (\overrightarrow{A_2B_2} \times \overrightarrow{A_2B_1}) \leqslant 0.\end{aligned} \quad (2)$$

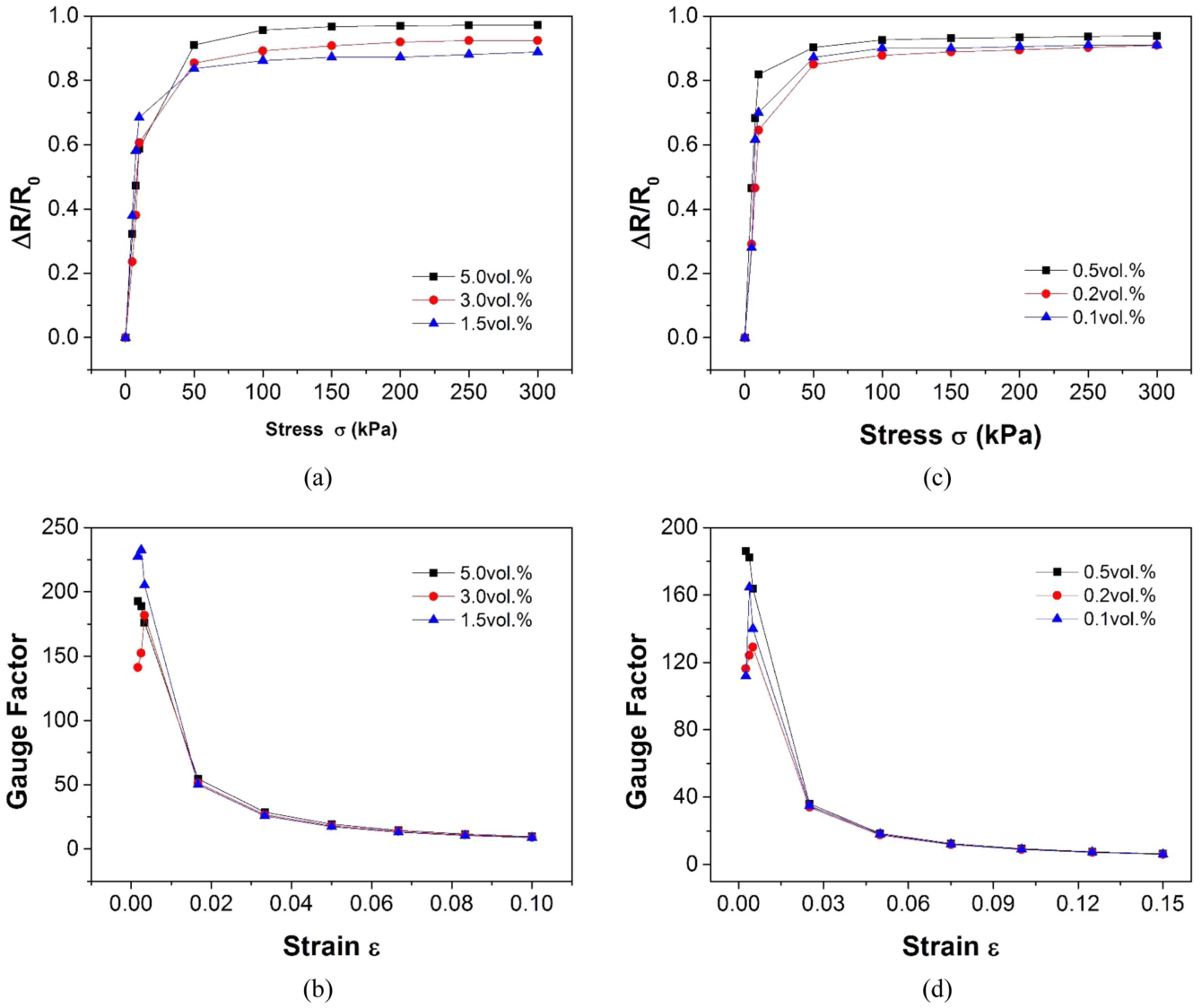

Figure 5. (a) Relative resistance change of CIPs–PDMS (cured under 0.2 T) as a function of stress. (b) Gauge factor of CIPs–PDMS (cured under 0.2 T) depended on strain. (c) Relative resistance change of CIPs–PDMS (cured under 1.0 T) as a function of stress. (d) Gauge factor of CIPs–PDMS (cured under 1.0 T) depended on strain.

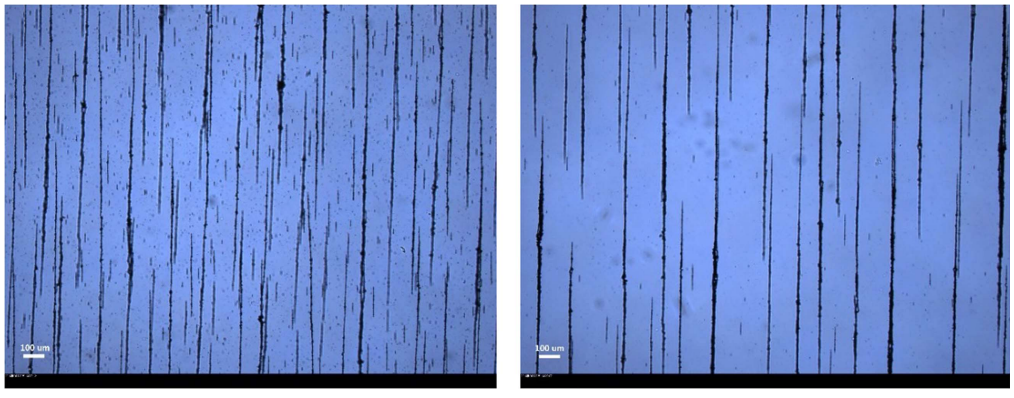

Figure 6. Lateral view of the CIP chains in the CIP–PDMS composites (CIPs 0.1 vol%) cured under various magnetic fields. (a) 0.2 T, (b) 1.0 T.

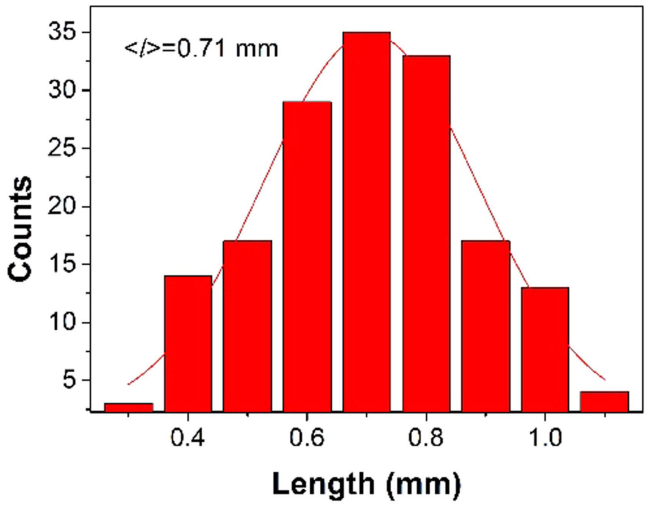

(a)

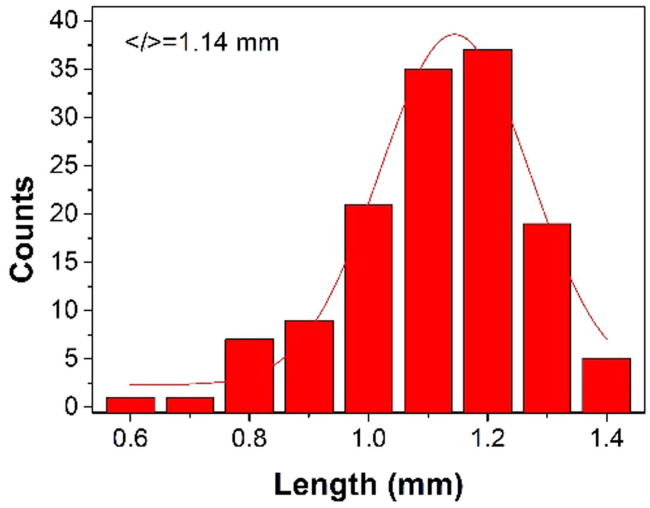

(b)

Figure 7. (a) Histogram for the length distribution of the conductive chains in the CIPs–PDMS composites cured under 0.2 T. (b) Histogram for the length distribution of the conductive chains in the CIPs–PDMS composites cured under 1.0 T. The histogram is fitted by a Gaussian distribution function (solid line).

Initially, each line segment is assigned a unique network number. If two line segments intersect, the minimum of their network number is set as their common number. In this way, small network numbers prevail. Finally, a spanning conductive network is identified when line segments connected to two opposite edges have common network number. To get a reliable percolation probability, the simulation should run for many times. If out of n simulations, k of them exist at least one spanning conductive network, then k/n is regarded as the percolation probability. For an acceptable accuracy, 100 Monte Carlo simulations are performed in this study to obtain each percolation probability. We also accept that the percolation probability >0.5 is an indicative of the existence of spanning conductive networks.

Based on the experiments, it is found that the percolation probability increases abruptly with the increase of the volume fraction of the CIPs indicating that there is an EPT exists. The EPT in this simulation is defined at the percolation probability equal to 0.5 (averaged over 100 simulations). In the 2D simulation cell, 100 line segments are distributed anisotropically. The line segments are assumed at a unified length that the EPT depends mainly on the average length of the stick-like fillers and the angle distribution [36]. The orientation of the line segments are limited by an angle θ with respect to a horizontal axis, $-5^\circ < \theta < 5^\circ$ corresponding to previous experimental observation. As shown in figure 8, the percolation probability curve versus the length L can be divided into three phases. Phase I, the percolation probability is almost equal to 0 when the length L is relatively small. Phase II, the percolation probability increases drastically with the increase of L and the percolation threshold occurs when $L = 0.83$ mm. Phase III, the percolation probability is always equal to 1 what means that there is at least one spanning network in the cell.

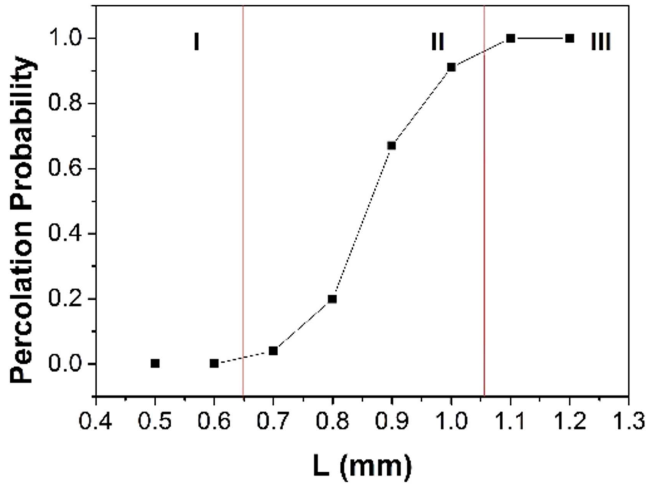

Figure 8. Percolation probability versus the length L for anisotropic stick percolation system.

The crucial parameter on the EPT is the length of the line segments. To evaluate the influence of curing magnetic field on the EPT of aligned CIPs–PDMS composites, the length L are set to be 0.71 and 1.14 mm in the simulations corresponding to CIPs–PDMS composites cured in 0.2 T and 1.0 T, respectively. It is clear to see from figure 9 that CIP chains with length $L = 1.14$ mm are easier to form spanning networks than that with length $L = 0.71$ mm. As shown in figure 10, at the length $L = 0.71$ mm, the percolation probability with a value of 0.5 is obtained at 177 CIP chains dispersed in the cell as well as that is obtained at 43 CIP chains dispersed at the length $L = 1.14$ mm. In the following we show how the numbers of chains dispersed in the matrix cell can be converted into particle volume fraction.

As shown in figure 11, assuming that the CIP chains arrange along the z-axis direction, View I and View II are the side view and the top view of the CIP chains respectively. In View I, N_{chain} CIP chains arrange in the z-axis direction, however, it can be considered approximately that the CIP chains distribute evenly in the x-axis direction. Therefore, in View II, the CIP chains can be considered into a square

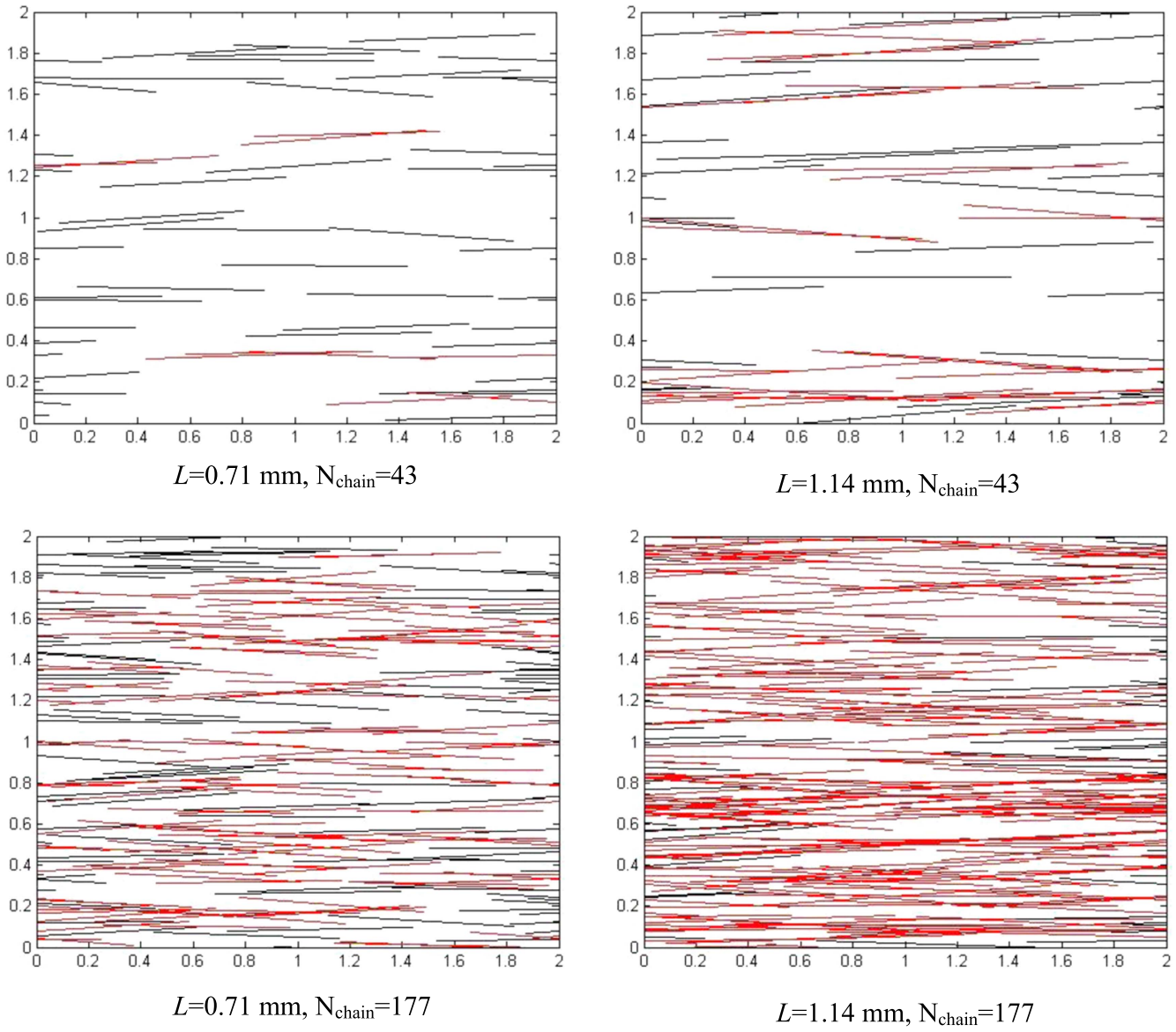

Figure 9. Examples of anisotropic stick percolation systems with different lengths L.

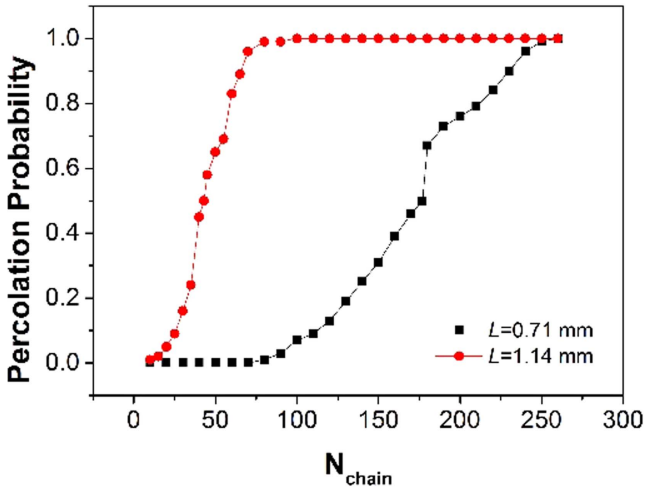

Figure 10. Percolation probability as a function of the amount of line segments with different lengths L.

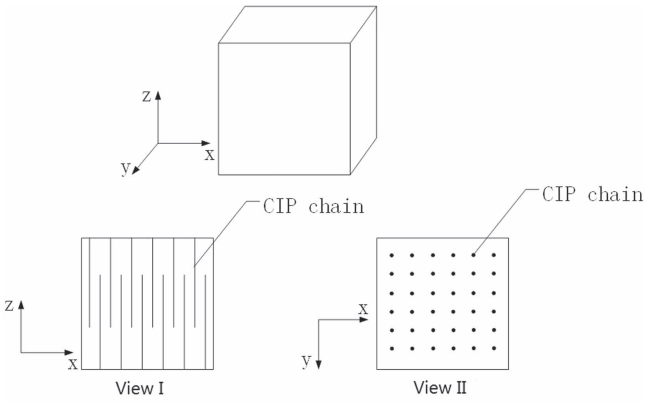

Figure 11. The microstructure sketch of the anisotropic CIPs–PDMS composites.

formation, and the number of the CIP chains is about $N_{chain}{}^2$, i.e. there are $N_{chain}{}^2$ CIP chains in the 3D cubic cell (side $a = 2$ mm). The volume fraction of the CIPs in the 3D cubic cell is described as follows

$$\varphi_{vol} = \frac{V_{CIP} \times N_{CIP} \times N_{chain}{}^2}{a^3}, \quad (3)$$

$$V_{CIP} = \frac{4}{3} \times \pi \times r^3, \quad (4)$$

$$N_{CIP} = \frac{L}{2 \times r}, \quad (5)$$

where φ_{vol} is the volume fraction of the CIPs, V_{CIP} is the volume of one CIP, N_{CIP} is the number of the CIPs in one CIP chain, a is the side length of the cell, r is the average radius of the CIPs, and L is the average length of the CIP chains. Substituting equations (4) and(5) into equation (3), we obtain equation (6) as follows

$$\varphi_{vol} = \frac{2 \times \pi \times r^2 \times L \times N_{chain}{}^2}{3 \times a^3}. \quad (6)$$

Using above method, the EPTs of the aligned CIPs–PDMS composites are calculated as 1.29 vol% and 0.12 vol% corresponding to the 177 CIP chains and 47 CIP chains, which represent the samples with average length of chains of 0.71 mm and 1.14 mm, respectively. These results are in good agreement with the measured EPT value of 1.49 vol% and 0.10 vol% for the CIPs–PDMS composites cured by a magnetic field of 0.2 and 1 T.

4. Conclusions

Alignment of carbon iron particles into PDMS under an external magnetic field can create anisotropic CIPs–PDMS conductive composites. The conductivity of these composite materials increases with the curing magnetic fields as well as the particle volume fractions. There is an EPT in which the conductivity of the CIPs–PDMS composites rapidly increases by many orders of magnitude. Both experimental and simulation studies show that CIPs–PDMS composites curing under an applied magnetic field of 1.0 T can significantly reduce the EPT as low as 0.10 vol% which has not been found in spherical particles filled conductive composites. This very low percolation behavior of anisotropic CIPs–PDMS composites could contribute to the chain-like structures of the particles. By examining two samples curing under magnetic fields of 0.2 and 1.0 T, it is found that the lengths of the CIP chains forming inside the matrix vary with magnetic field strengths. The higher magnetic field applies, the longer the CIP chains are.

Based on the morphological observation of the composite structures, a two-dimensional stick percolation model for the CIPs–PDMS composites has been established. A numerical algorithm is developed to check whether two sticks intersect and Monte Carlo simulations are performed to obtain the percolation probability. The simulation results in prediction of the values of EPTs are close to that of experimental measurements. It demonstrates that the low percolation behavior of CIPs–PDMS composites is due to the average length of particle chains forming by external magnetic field.

Meanwhile, the effects of compressive strain on the electrical properties of CIPs–PDMS composites are also investigated. The strain sensitivity depends on filler volume fraction and decreases with the increasing of compressive strain. It has been found that the composites containing a small amount of CI particles curing under a magnetic field exhibit a high strain sensitivity of over 150.

This work provides a method to create conductive composite with low percolation threshold and high piezoresistivity by mixing alignment of carbon iron into polydimethylsiloxane. The CIPs–PDMS composites can be used as smart materials to monitor force or deformation. The future research will focus on improving the composite properties in piezoresistivity and conductivity so that it can be used in sensing.

Acknowledgments

This work was supported by the National Nature Science Foundation of the People's Republic of China (NO.11572320), and Chongqing City Basic and Frontier Research Project (cstc2015jcyjBX0135).The authors would like to thank the Anhui Provincial Natural Science Foundation for its partial financial support (NO.1608085ME96) as well as the Changzhou applied basic research program (CJ20159005).

References

[1] Canavese G, Stassi S, Stralla M and Pirri C F 2012 Stretchable and conformable metal–polymer piezoresistive hybrid system *Sensors Actuators* A **186** 191–7
[2] Kato Y and Mukai T 2008 Tactile sensor without wire and sensing element in the tactile region using new rubber material *INTECH Open Access Publisher*
[3] Stassi S, Cauda V, Canavese G and Pirri C F 2014 Flexible tactile sensing based on piezoresistive composites: a review *Sensors* **14** 5296–332
[4] Lu H, Gou J, Leng J and Du S 2011 Magnetically aligned carbon nanotube in nanopaper enabled shape-memory nanocomposite for high speed electrical actuation *Appl. Phys. Lett.* **98** 174105
[5] Lu H, Liang F and Gou J 2011 Nanopaper enabled shape-memory nanocomposite with vertically aligned nickel nanostrand: controlled synthesis and electrical actuation *Soft Matter.* **7** 7416–23
[6] Ghafoorianfar N, Wang X and Gordaninejad F 2014 Combined magnetic and mechanical sensing of magnetorheological elastomers *Smart Mater. Struct.* **23** 055010
[7] Wang X, Gordaninejad F, Calgar M, Liu Y, Sutrisno J and Fuchs A 2009 Sensing behavior of magnetorheological elastomers *J. Mech. Design* **131** 091004
[8] Bica I, Anitas E M, Bunoiu M, Vatzulik B and Juganaru I 2014 Hybrid magnetorheological elastomer: influence of magnetic field and compression pressure on its electrical conductivity *J. Ind. Eng. Chem.* **20** 3994–9

[9] Abyaneh M K and Kulkarni S K 2008 Giant piezoresistive response in zinc–polydimethylsiloxane composites under uniaxial pressure *J. Phys. D: Appl. Phys.* **41** 135405
[10] Abyaneh M K, Ekar S and Kulkarni S K 2012 Piezoresistivity and mechanical behavior of metal–polymer composites under uniaxial pressure *J. Mater. Sci. Res.* **1** 50–8
[11] Jung J, Kim M, Choi J K, Park D W and Shim S E 2013 Piezoresistive effects of copper-filled polydimethylsiloxane composites near critical pressure *Polymer* **54** 7071–9
[12] Bloor D, Donnelly K, Hands P J, Laughlin P and Lussey D 2005 A metal–polymer composite with unusual properties *J. Phys. D: Appl. Phys.* **38** 2851–60
[13] Shang S, Song G, Chu X, Zhang L and Chang F 2014 AC and DC behavior of finger-sensing metal/polymer composites at various pressures *Compos. Sci. Technol.* **97** 115–20
[14] Shang S, Zhou X, Chang F and Guo C 2012 Critical electrical behaviors of finger-sensing metal/polymer composites near the percolation threshold *Appl. Phys. Lett.* **101** 211904
[15] Mietta J L, Jorge G and Negri R M 2014 A flexible strain gauge exhibiting reversible piezoresistivity based on an anisotropic magnetorheological polymer *Smart Mater. Struct.* **23** 085026
[16] Mietta J L, Ruiz M M, Antonel P S, Perez O E, Butera A, Jorge G and Negri R M 2012 Anisotropic magnetoresistance and piezoresistivity in structured Fe_3O_4–silver particles in PDMS elastomers at room temperature *Langmuir* **28** 6985–96
[17] Jang S H and Yin H M 2015 Effect of aligned ferromagnetic particles on strain sensitivity of multi-walled carbon nanotube/polydimethylsiloxane sensors *Appl. Phys. Lett.* **106** 141903
[18] Boudenne A, Mamunya Y, Levchenko V, Garnier B and Lebedev E 2015 Improvement of thermal and electrical properties of silicone–Ni composites using magnetic field *Eur. Polym. J.* **63** 11–9
[19] Jang S H, Park Y L and Yin H 2016 Influence of coalescence on the anisotropic mechanical and electrical properties of nickel powder/polydimethylsiloxane composites *Materials* **9** 239
[20] Goc K, Gaska K, Klimczyk K, Wujek A, Prendota W, Jarosinski L and Kapusta C 2016 Influence of magnetic field-aided filler orientation on structure and transport properties of ferrite filled composites *J. Magn. Magn. Mater.* **419** 345–53
[21] Su J, Mirzaee I, Gao F, Liu X, Charmchi M, Gu Z and Sun H 2014 Magnetically assembling nanoscale metal network into phase change material-percolation threshold reduction in paraffin using magnetically assembly of nanowires *J. Nanotechnol. Eng. Med.* **5** 031005
[22] Sumfleth J, Buschhorn S T and Schulte K 2011 Comparison of rheological and electrical percolation phenomena in carbon black and carbon nanotube filled epoxy polymers *J. Mater. Sci.* **46** 659–69
[23] White S I, Mutiso R M, Vora P M, Jahnke D, Hsu S, Kikkawa J M and Winey K I 2010 Electrical percolation behavior in silver nanowire–polystyrene composites: simulation and experiment *Adv. Funct. Mater.* **20** 2709–16
[24] Gelves G A, Lin B, Sundararaj U and Haber J A 2006 Low electrical percolation threshold of silver and copper nanowires in polystyrene composites *Adv. Funct. Mater.* **16** 2423–30
[25] Bryning M B, Islam M F, Kikkawa J M and Yodh A G 2005 Very low conductivity threshold in bulk isotropic single-walled carbon nanotube-epoxy composites *Adv. Mater.* **17** 1186–91
[26] Krause B, Boldt R, Häußler L and Pötschke P 2015 Ultralow percolation threshold in polyamide 6.6/MWCNT composites *Compos. Sci. Technol.* **114** 119–25
[27] Hu N, Masuda Z, Yan C, Yamamoto G, Fukunaga H and Hashida T 2008 The electrical properties of polymer nanocomposites with carbon nanotube fillers *Nanotechnology* **19** 215701
[28] Vasanthkumar M S, Bhatia R, Arya V P, Sameera I, Prasad V and Jayanna H S 2014 Characterization, charge transport and magnetic properties of multi-walled carbon nanotube-polyvinyl chloride nanocomposites *Physica* E **56** 10–6
[29] Du F, Fischer J E and Winey K I 2005 Effect of nanotube alignment on percolation conductivity in carbon nanotube/polymer composites *Phys. Rev.* B **72** 121404
[30] Jang H K, Jin J E, Choi J H, Kang P S, Kim D H and Kim G T 2015 Electrical percolation thresholds of semiconducting single-walled carbon nanotube networks in field-effect transistors *Phys. Chem. Chem. Phys.* **17** 6874–80
[31] Zheng X, Forest M G, Vaia R, Arlen M and Zhou R 2007 A strategy for dimensional percolation in sheared nanorod dispersions *Adv. Mater.* **19** 4038–43
[32] Rahatekar S S, Shaffer M S and Elliott J A 2010 Modelling percolation in fibre and sphere mixtures: routes to more efficient network formation *Compos. Sci. Technol.* **70** 356–62
[33] Arenhart R G, Barra G M O and Fernandes C P 2016 Simulation of percolation threshold and electrical conductivity in composites filled with conductive particles: effect of polydisperse particle size distribution *Polym. Compos.* **37** 61–9
[34] Mietta J L, Negri R M and Tamborenea P I 2014 Numerical simulations of stick percolation: application to the study of structured magnetorheological elastomers *J. Phys. Chem.* C **118** 20594–604
[35] Zeng X, Xu X, Shenai P M, Kovalev E, Baudot C, Mathews N and Zhao Y 2011 Characteristics of the electrical percolation in carbon nanotubes/polymer nanocomposites *J. Phys. Chem.* C **115** 21685–90
[36] Lu W, Chou T W and Thostenson E T 2010 A three-dimensional model of electrical percolation thresholds in carbon nanotube-based composites *Appl. Phys. Lett.* **96** 223106